Nanocatalysts: Properties and applications

Gaikwad, A.V.

Publication date
2009

Chapter 3

Growing anisotropic gold nanoparticles in organic media

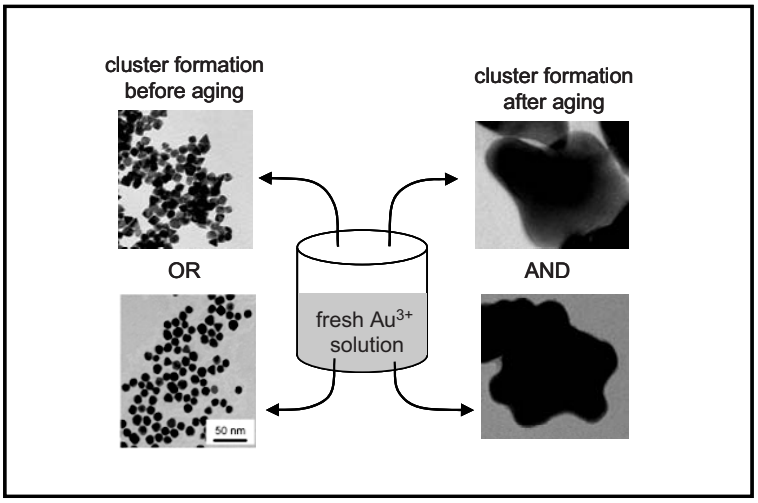

Part of this work is published as "Matter of Age: Growing Anisotropic Gold Nanocrystals in Organic Media", A. V. Gaikwad, P. G. Verschuren, G. Rothenberg and E. Eiser, *Phys. Chem. Chem. Phys.*, **2008**, *10*, 951.

Introduction

Synthesising metal nanoparticles using "bottom-up" techniques is attracting much attention due to their applications in catalysis,[1-4] optoelectronics,[5, 6] biological labeling,[7] fuel cells[8] and materials science.[9] Nanometric metal crystals display unique physico-chemical properties that stem from their size and shape. Several studies have achieved excellent control over particle size for both metallic and semiconductor nanocrystals. However, although scientists have managed to make a variety of nanosized crystal shapes including rods,[10-13] triangular prisms,[14-17] disks,[18-20] and even cubes,[21] understanding the factors that govern shape control remain a challenge.[22]

In many applications, crystal anisotropy is a key factor. Nanocrystals with different shapes exhibit different optical and electronic properties, and consequently a variation in the surface-plasmon resonance. To exploit those activities, branched and multipod structures have been made. The most common recipe for making such crystals is the seeded growth of anisotropic particles in water.[23-28] The formation of triangular, hexagonal, decahedral and cubic particles, as well as nanowires, was also reported in DMF and pyridine.[29-32] In all those studies, the interaction of the stabiliser with metal ions and the form of the seeds play a crucial role in controlling the final particles' size and morphology (for example, El-Sayed et al. showed that the particles' shape can be controlled by changing the capping ratio of metal ions to stabiliser [33-35]).

Recently, we studied the preparation and catalytic applications of various metal nanoparticles (Pd, Ru, Ni, Ag, and Cu) in DMF and toluene using tetraoctyl ammonium carboxylate salts as reducing and stabilizing agents.[36-38] In all these cases, we obtained spherical particles. Extending this work to gold nanocrystals, we were surprised to find, using the same synthesis method, a variety of nanocrystal shapes. Although different well defined shapes of gold nanocrystals are reported, the formation of branched particles for this particular system in DMF was never reported. We thus began to investigate the cause for these different morphologies. In contrast to aqueous solutions, where a reducing agent is needed for initiating the nanoparticle formation, DMF and formamide can themselves reduce silver and gold salts partially or completely.[39-43] In the present work, we investigate the factors that govern the formation of anisotropic gold particles in DMF using tetraoctylammonium ions as a stabiliser. We show that precursor aging and reducing agent concentration influence the concentration of Au^{3+} and Au^{+} ions. This in turn affects the rates of Au^{0} seed formation and nanoparticle growth.

Experimental

Materials and instrumentation. In situ UV-visible measurements were performed using a Hewlett Packard 8453 spectrophotometer with a diode array detector. The quartz cuvette (Hellma Benelux, approximately 3.5 ml, path length 1 cm) was mounted on a sample holder with controlled heating (Neslab constant temperature bath) and stirring (compressed air was used to rotate the stirrer at the bottom of the cuvette). The recorded wavelength range was 190–1100 nm, at 1 nm resolution. TEM images were obtained with a JEOL model JEM-1200 EXII instrument, operated at an accelerating voltage of 120 kV. Unless stated otherwise, chemicals were purchased from commercial firms (>98% pure) and used as received. All solvents were degassed for 10 min with dry N_2 prior to use. GC-MS measurements were done using Agilent 6890/5793 instrument (with HP-5 MS crosslink phase column, 30 m length, internal diameter 0.25 mm, film thickness 0.25 μm). IR spectra were measured using Bruker Vortex 70 instrument using $CaCl_2$ cell. Karl-fisher titrations were performed using a Mettler Toledo DL 36 KF coulometer instrument. 250 ml of Hydraneal water standard (0.1% H_2O) was used as internal standard. Cyclic voltammograms were recorded with a PAR EG&G model 283 potentiostat, using an airtight single-compartment cell placed in a Faraday cage. The working electrode was a Pt microdisk (0.42 mm^2 apparent surface area), polished with a 0.25 μm diamond paste between the scans. Coiled Pt and Ag wires served as an auxiliary and pseudo reference electrode, respectively. The concentration of the analyte was 1 mM. Ferrocene (Fc) was used as the internal standard. The supporting electrolyte, $[Bu_4N][PF_6]$, was recrystallized twice from absolute EtOH and dried overnight under vacuum at 80 °C before use.

Procedure for *in situ* monitoring of Au nanoparticles and anisotropic particles
Four types of samples (**A**, **B**, **C**, and **D**) were prepared

Sample A. A quartz cuvette equipped with a rubber septum and a magnetic stirrer was evacuated and refilled with N_2. It was charged with 2 ml of a 0.5 mM $AuCl_3$/DMF aged solution. Then, 75 μl of 100 mM of TOAF in DMF was added in one portion into the cuvette and stirred and heated at 65 °C for 1 h under N_2. UV-vis spectra were recorded every 1.1 min for 60 min.

Sample B was prepared using the same method, but using 2 ml of a fresh 0.5 mM $AuCl_3$/DMF solution and 60 μl of 100 mM of TOAF/DMF was added. The sample was then heated to 65 °C and stirred under N_2 for 1 h.

Sample C Sample **C**: For control experiments 2 ml of fresh 0.5 mM AuCl solution in DMF was prepared that contains only Au^{+} ions in contrast to sample **B** containing mainly Au^{3+} ions. As in sample **B**, immediately after dissolution 60 µl of 100 mM TOAF in DMF was added, and the mixture was heated to 65 °C and stirred under N_2 for 1 h.

Sample D 2 ml of fresh 0.5 mM $AuCl_3$ solution in DMF was mixed with 50 µl of 200 mM TOAF in DMF then heated and stirred for 1 h under the same conditions as in sample **A** and **B**. This experiment was repeated with 60 µl and 70 µl of 200 mM TOAF in DMF.

Results and discussion

We started by synthesizing gold nanoparticles following the method of Reetz and Maase,[44] using $AuCl_3$ in DMF as salt precursor solution and tetra-*n*-octylammonium formate (TOAF) as reducing and stabilising agent. This method was expected to yield spherical nanoparticles with a narrow size distribution. For sample **A** the colourless $AuCl_3$ precursor solution was prepared a day in advance, a fact that at the time seemed unimportant and innocuous. After nanoparticle formation this sample appeared blue and clear in transmission but brown and turbid in reflection (we did not observe any aggregate precipitation). In order to characterise the cluster growth we monitored the evolution of sample **A** *in situ* using UV-visible spectroscopy. At $t = 0$, the moment the reducing agent was added we observed neither the typical absorption peak of the Au^{3+} ion precursor (λ = 322 nm) nor the surface-plasmon peak typical for Au spherical nanocrystals ($\lambda \sim 550$ nm). Instead, we observed the evolution of a surface plasmon peak at *ca.* 790 nm with a shoulder at 590 nm (Figure 1), typical for samples containing anisotropic nanoparticles.[45, 46] The reaction was completed after one hour rendering sample **A** stable for over four weeks at 25 ºC. Further characterisation of sample **A** by HRTEM showed indeed variously shaped particles, roughly 40–80 nm in diameter (Figure 2). A close up view showed different particle shapes including bipods, tripods, tetrapods, and branched nanoparticles.

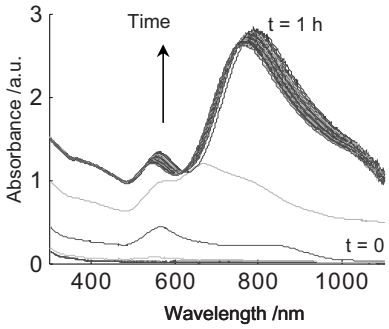

Figure 1. UV-visible spectra of anisotropic Au-nanoparticle formation in sample **A**. The lowest curve indicates the starting situation, $t = 0$, of the nanoparticle growth.

To investigate this phenomenon further we prepared gold nanoparticles from a freshly prepared $AuCl_3$ precursor solution (sample **B**). Here, TOAF was immediately added to the fresh solution and kept at 65 °C for 1 h, like in sample **A**. Monitoring this reaction using UV-visible spectroscopy, initially (t = 0) we observed only the absorption peak of the free Au^{3+} ions (Figure 3). However, within a few minutes this Au^{3+} peak decreased to zero, followed by a clear surface plasmon peak emerging at ~ 600 nm. A TEM analysis confirmed that sample **B** contains mainly spherical particles, with a narrow size distribution of 14 nm ± 2.0 nm. To ensure reproducibility, triplicate experiments were carried out in each case. In all cases, freshly prepared solutions of $AuCl_3$ in DMF lead to the formation of spherical gold nanocrystals with an average diameter of ~15 nm. For control we also repeated the reduction experiments with aged (colourless) precursor samples following the preparation protocol for sample **A**. Once again we obtained anisotropic gold nanoparticles with similar shapes and size (Figure 2, top) as those shown in Figure 2.

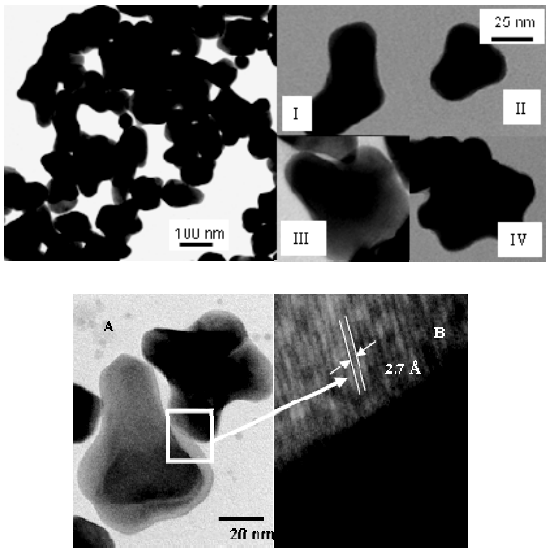

Figure 2. (top left) TEM images of branched particles prepared using an aged $AuCl_3$ precursor solution in DMF – sample **A**; (top right) Close ups of TEM images of different shaped particles that can be distinguished: (I) bipod, (II) tripod, (III) tetrapod, and (IV) branched gold nanocrystals. (Bottom) HRTEM image of branched gold nanocrystals (sample **A**). (B) Blow up of the white square in image (A). The two parallel lines indicate the packing distance between two hexagonally packed dense Au-planes.

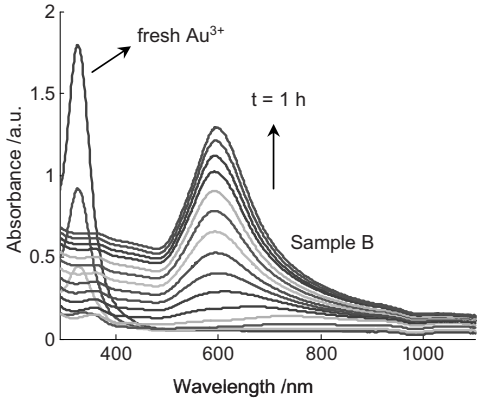

Figure 3. (top) Time-resolved *in situ* UV-visible spectra of precursor reduction and nanoparticles formation using the freshly prepared $AuCl_3$ precursor solution **B**.

To understand this, we first investigated the aging behaviour of $AuCl_3$ in DMF prior to the addition of any reducing agent. Figure 4 shows the UV-visible absorption spectra of $AuCl_3$ (0.5 mM) in DMF at 25 ºC over 20 h under an inert atmosphere. Although no external reducing agent was present, we observed a clear disappearance of the Au^{3+} ion peak at 322 nm. It was reported that DMF reduces Au^{3+} ions under reflux conditions in the presence of a stabilising agent such as (poly)vinylpyrrolidone, giving spherical gold nanoparticles,[43] so we presumed that some reduction could also occur at room temperature. This reaction, however, requires also at least one equivalent of water (eqs *1* and *2*).[47] Karl-Fischer titrations confirmed that the DMF we used contained 0.04% water, or 44 equivalents, sufficient for reducing the Au^{3+} ions to Au^{+} ions and Au^{0} atoms. Moreover, while the fresh $AuCl_3$ solution in DMF was neutral, the aged precursor solution was acidic (pH = 4.5), supporting the formation of carbamic acid and H^{+} ions via eqs *1* or *2*.

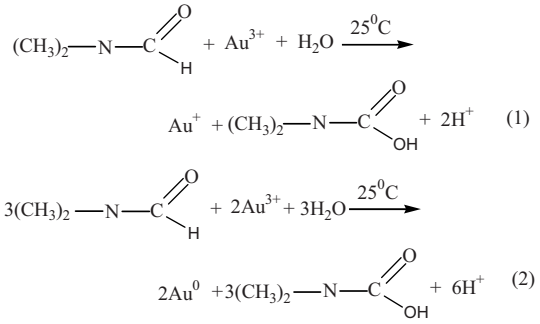

Whether Au^{3+} partially reduces to Au^{+} or completely to Au^{0} in DMF is unknown. Pradeep and co-workers hypothesised that Au^{3+} reduces completely to Au^{0}, in a similar fashion to Ag, thereby producing carbamic acid.[48] Carbamic acid is unstable in DMF and readily decomposes to $(CH_3)_2NH$ and CO_2. Similar to Tom *et al.*[48] we performed infra red spectroscopy (IR) and gas chromatography-mass spectroscopy (GC-MS). However, their weak signal was dominated by the strong contributions from DMF. We surmised that our aged $AuCl_3$ precursor solution contained both Au^{+} and Au^{0} species. This was confirmed by cyclic voltammetry studies of aged and fresh gold precursor solutions. While the fresh solution showed two reduction peaks for $Au^{3+} \rightarrow Au^{+}$ (E_v = 0.49 V) and $Au^{+} \rightarrow Au^{0}$ (E_v = 0.95 V) respectively, the aged solution showed only one, corresponding to $Au^{+} \rightarrow Au^{0}$ (E_v = 1.05 V; the cyclic voltagrams are included in the supporting information, Figure 5). Freshly dissolved AuCl-DMF solutions also showed only one reduction peak, agreeing well with our observations in aged solutions. Based on these findings we hypothesise that

next to Au^{+} ions the presence of Au^{0} atoms or neutral gold seed of less than 1nm in size is necessary to initiate the formation of gold nanocrystals in DMF

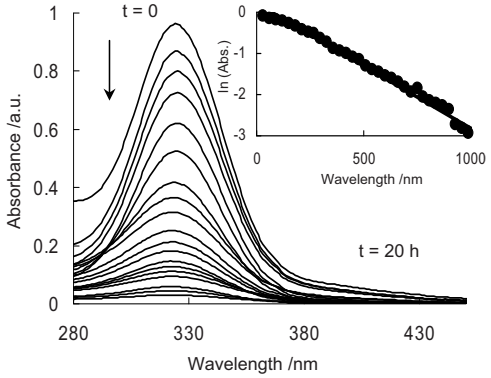

Figure 4. Time-resolved UV-visible spectra of the reduction of Au^{3+} ions in DMF at 25 ºC. The inset shows the rate of reduction in terms of decrease in absorbance of Au^{3+} at λ_{max} = 322 nm versus time.

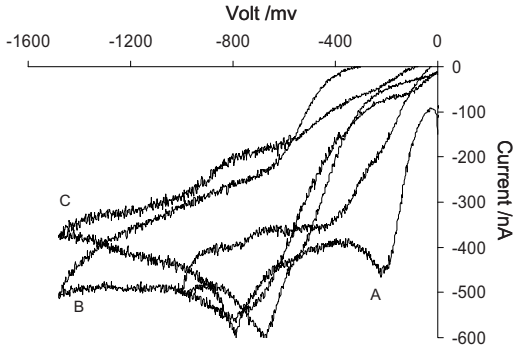

Figure 5. Cyclic voltamograms of fresh $AuCl_3$ (A), fresh AuCl (B), and aged $AuCl_3$ (C) solution in DMF. The different value for E_v for Au^{+} in the fresh and aged solution may arise from the presence of Au^{0} seeds in latter solution.

To test our hypothesis we then prepared sample **C**, starting from fresh AuCl precursor solutions in DMF containing only Au^{+} ions similar to the aged solution, and using the same amount of the reducing and stabilising agent TOAF as in sample **B**. As expected we did not observe any nanoparticle formation. The reduction potential of Au^{+} ions to Au^{0} atoms is higher than that of Au^{3+} ions.[38] This showed that the aged solution

contained both Au^{+} ions and Au^{0} that can form a complex with DMF. Gold nanoparticles have a high electron affinity and can strip off electrons from the DMF molecules.[49] The resulting complexes act as seeds for further reduction of Au^{+} ions (the so-called aurophilic effect[50]) and grow to give branched particles when the reducing agent TOAF was added, as demonstrated in Figure 1. Such particle growth in liquid media involves mainly two factors: One is the influence of the capping agent, that controls the growth on the various crystal facets.[51] The second is the rate of supply of Au^{0} to the crystal planes of the growing seed particles. A third influence can arise due to surface autocatalytic reduction of Au^{+} ions at the gold nanocrystals surface, but may not be as effective as the first two, as it is limited to a rather small available surface area.[52-55] Thus, the shape and size of the seed play an important role.[56] To understand the effect of the second factor we compared the rate of increase in intensity of the surface plasmon peaks in samples **A** and **B** (Figure 6).

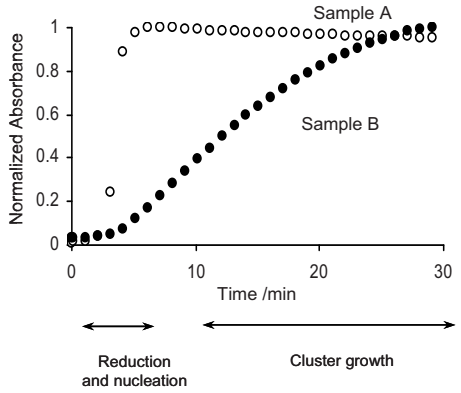

Figure 6. Change in the normalised surface-plasmon absorption of sample **A** (500 – 650 nm) and **B** (500 – 700 nm) versus time. In each case the range of wavelengths was used to compensate for the peak shift with particle growth.

Comparing the aged precursor (sample **A**) to the fresh precursor (sample **B**), we see that in **A** the surface plasmon appears fast and the absorption increases, reaching a plateau after ~ 5 min. Conversely, **B** exhibits a prolonged reduction period reaching a plateau only after 25 min. Sample **A** shows almost no induction period. This probably reflects the fact that some of the Au^{3+} ions are already reduced to Au^{0} atoms or Au^{1+} ions in DMF, and subsequently form sub-nanometer seed particles that are too small to show a plasmon peak.[57] When the external reducing agent is added (at $t = 0$), further reduction of the remaining Au^{+} ions and subsequent particle growth are fast, and the different reduction

rates at the various crystal surfaces ultimately yield different crystal shapes (*vide infra*). Conversely, in case **B**, the nanoparticles grow uniformly in all directions and the increase of the surface plasmon resonance shows a typical S-shaped curve. This type of curve agrees well with the results of Gan *et al*.[41] The induction period denotes the time to reduce Au^{3+} to Au^0 atoms that nucleate and form sub-nanometric seed particles.[41, 58]

To study this effect of rate generation of Au^0 atoms on the nanoparticles morphology, we reduced a fresh Au^{3+} solution using higher TOAF concentrations than in sample **B** (sample **D**). Here we obtained high yields of cubes (60 %), prisms (30 %), and spherical particles (10 %) of 20–30 nm in size (Figure 7). Importantly, we did not observe any branched particles. We conclude that the shape of the gold nanoparticles depends on the reducing agent concentration as well as on the interaction of the stabiliser with the different crystal surfaces.[59] In fact, a higher ratio of reducing agent to Au^{3+} ions causes monomer super saturation. This leads to a simultaneous nucleation and growth process resulting in anisotropic particles, especially with "soft metals" like gold. Conversely, hard metal nanocrystals such as Pd, Pt and Cu yield mainly spherical nanoparticles, their size depending only on the concentration of TOAF as reducing and stabilising agent.[58]

The formation of multipod shapes is associated with rate of supply of Au^0 atoms to *(1,1,1)*, *(1,1,0)* and *(1,0,0)* crystal planes.[24, 60] The corresponding surface energy [61] increases in the order $Au_{(1,1,1)} < Au_{(1,0,0)} < Au_{(1,1,0)}$. The tetraoctylammonium species adsorb preferentially on the low-energy *(1,1,1)* surface, leaving the other surfaces open for further crystal growth. The formation of spherical, cubic, prism, or branched shapes depends on the local concentration of Au^0 atoms. In the case of sample **B**, where the formation of Au^0 atoms is slow and hence the local concentration is low, the rate of association/dissociation of the tetraoctylammonium species is similar to that of the Au^0 atoms, resulting in spherical particles. Conversely, sample **D** has a high concentration of Au^0, which causes an imbalance that promotes growth on the available *(1,1,0)* and *(1,0,0)* planes, resulting in cubes and prisms, respectively. In case of sample **A**, the crystals grow simultaneously on the *(1,0,0)* and the *(1,1,0)* planes, resulting in multipod structures.[25] Finally, we note that the preferential adsorption of halide counterions onto the different crystallographic surfaces of the gold particles may have an influence on the shape morphism.[62, 63] In the present study this influence can be neglected as we only considered only Cl^- counterions.

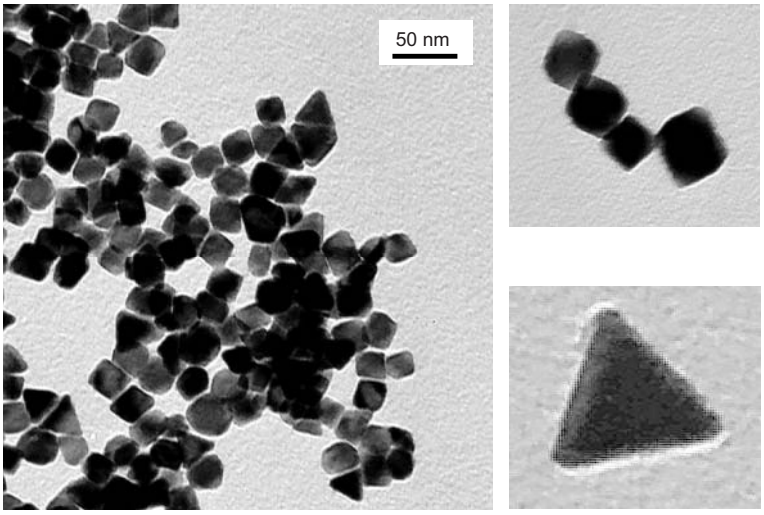

Figure 7. TEM images of nanoprisms and nanocubes prepared using fresh $AuCl_3$ precursor solution with higher TOAF concentration (sample **D**, 60 % cubic, 30 % triangular and 10 % spherical particles, based on 100 particles counted).

Conclusion

The shape and size of gold nanoparticles depend strongly on the concentration of the reducing agent and the presence of sub-nanometric seed particles. While using DMF as a solvent one should take into account that the solvent DMF can already reduce Au^{3+} ions to Au^{+} /Au^{0} (even though this process is much slower than the reduction in the presence of TOAF). The reduction processes of Au^{+} and Au^{3+} are distinct, and can be followed using cyclic voltammetry. Changing the concentration of the reducing agent and controlling the freshness of the precursor solution, gives access to isotropic or anisotropic gold nanoparticles (including cubes, prisms, and branched particles).

References

[1] A. Roucoux, J. Schulz, H. Patin, *Chem. Rev.*, **2002**, *102*, 3757.

[2] H. Bönnemann, R. M. Richards, *Eur. J. Inorg. Chem.*, **2001**, 2455.

[3] C. R. LeBlond, A. T. Andrews, Y. Sun, J. R. Sowa, Jr., *Org. Lett.*, **2001**, *3*, 1555.

[4] B. D. Chandler, L. H. Pignolet, *Catal. Today*, **2001**, *65*, 39.

[5] P. V. Kamat, *J. Phys. Chem. B*, **2002**, *106*, 7729.

[6] C. J. Murphy, T. K. Sau, A. M. Gole, C. J. Orendorff, J. Gao, L. Gou, S. E. Hunyadi, T. Li, *J. Phys. Chem. B*, **2005**, *109*, 13857.

[7] S. R. Nicewarner-Pena, R. Griffith Freeman, B. D. Reiss, L. He, D. J. Pena, I. D. Walton, R. Cromer, C. D. Keating, M. J. Natan, *Science*, **2001**, *294*, 137.

[8] S. S. C. Chuang, *Catalysis*, **2005**, *18*, 186.

[9] S. Nie, S. R. Emory, *Science*, **1997**, *275*, 1102.

[10] S. Link, M. A. El-Sayed, *J. Phys. Chem. B*, **1999**, *103*, 8410.

[11] Y.-Y. Yu, S.-S. Chang, C.-L. Lee, C. R. C. Wang, *J. Phys. Chem. B*, **1997**, *101*, 6661.

[12] X. Peng, U. Manna, W. Yang, J. Wickham, E. Scher, A. Kadavanich, A. P. Allvisatos, *Nature*, **2000**, *404*, 59.

[13] N. R. Jana, L. Gearheart, C. J. Murphy, *J. Phys. Chem. B*, **2001**, *105*, 4065.

[14] R. Jin, Y. Cao, C. A. Mirkin, K. L. Kelly, G. C. Schatz, J. G. Zheng, *Science*, **2001**, *294*, 1901.

[15] Y. Sun, B. Mayers, Y. Xia, *Nano Lett.*, **2003**, *3*, 675.

[16] S. Chen, D. L. Carroll, *Nano Lett.*, **2002**, *2*, 1003.

[17] G. S. Metraux, Y. C. Cao, R. Jin, C. A. Mirkin, *Nano Lett.*, **2003**, *3*, 519.

[18] M. Maillard, S. Giorgio, M. P. Pileni, *Adv. Mater.*, **2002**, *14*, 1084.

[19] V. F. Puntes, D. Zanchet, C. K. Erdonmez, A. P. Alivisatos, *J. Am. Chem. Soc.*, **2002**, *124*, 12874.

[20] M. Maillard, P. Huang, L. Brus, *Nano Lett.*, **2003**, *3*, 1611.

[21] Y. G. Sun, Y. N. Xia, *Science*, **2002**, *298*, 2176.

[22] C. J. Murphy, *Science*, **2002**, *298*, 2139.

[23] E. Hao, R. C. Bailey, G. C. Schatz, J. T. Hupp, S. Li, *Nano Lett.*, **2004**, *4*, 327.

[24] T. K. Sau, C. J. Murphy, *J. Am. Chem. Soc.*, **2004**, *126*, 8648.

[25] S. H. Chen, Z. L. Wang, J. Ballato, S. H. Foulger, D. L. Carroll, *J. Am. Chem. Soc.*, **2003**, *125*, 16186.

[26] C.-H. Kuo, M. H. Huang, *Langmuir*, **2005**, *21*, 2012.

[27] C. L. Nehl, H. Liao, J. H. Hafner, *Nano Lett.*, **2006**, *6*, 683.

[28] M. Yamamoto, Y. Kashiwagi, T. Sakata, H. Mori, M. Nakamoto, *Chem. Mater.*, **2005**, *17*, 5391.

[29] T. C. Deivaraj, N. L. Lala, J. Y. Lee, *J. Coll. Int. Sci.*, **2005**, *289*, 402.

[30] Y. Chen, X. Gu, C.-G. Nie, Z.-Y. Jiang, Z.-X. Xie, C.-J. Lin, *Chem. Comm.*, **2005**, 4181.

[31] M. Giersig, I. Pastoriza-Santos, L. M. Liz-Marzán, *J. Mater. Chem.*, **2004**, *14*, 607.

[32] A. Sanchez-Iglesias, I. Pastoriza-Santos, J. Perez-Juste, B. Rodriguez-Gonzalez, F. J. G. de Abajo, L. M. Liz-Marzan, *Adv. Mater.*, **2006**, *18*, 2529.

[33] T. S. Ahmadi, Z. L. Wang, T. C. Green, A. Henglein, M. A. ElSayed, *Science*, **1996**, *272*, 1924.

[34] B. Nikoobakht, M. A. El-Sayed, *Chem. Mater.*, **2003**, *15*, 1957.

[35] S. Eustis, M. A. El-Sayed, *Chem. Soc. Rev.*, **2006**, *35*, 209.

[36] L. Durán Pachón, J. H. van Maarseveen, G. Rothenberg, *Adv. Synth. Catal.*, **2005**, *347*, 811.

[37] M. B. Thathagar, J. Beckers, G. Rothenberg, *J. Am. Chem. Soc.*, **2002**, *124*, 11858.

[38] J. Wang, H. F. M. Boelens, M. B. Thathagar, G. Rothenberg, *ChemPhysChem*, **2004**, *5*, 93.

[39] I. Pastoriza-Santos, L. M. Liz-Marzan, *Pure Appl. Chem.*, **2000**, *72*, 83.

[40] A. Sarkar, S. Kapoor, T. Mukherjee, *J. Phys. Chem. B*, **2005**, *109*, 7698.

[41] M. Y. Han, C. H. Quek, W. Huang, C. H. Chew, L. M. Gan, *Chem. Mater.*, **1999**, *11*, 1144.

[42] I. Pastoriza-Santos, L. M. Liz-Marzan, *Langmuir*, **1999**, *15*, 948.

[43] I. Pastoriza-Santos, L. M. Liz-Marzan, *Langmuir*, **2002**, *18*, 2888.

[44] M. T. Reetz, M. Maase, *Adv. Mater.*, **1999**, *11*, 773.

[45] S. Underwood, P. Mulvaney, *Langmuir*, **1994**, *10*, 3427.

[46] C. S. Weisbecker, M. V. Merritt, G. M. Whitesides, *Langmuir*, **1996**, *12*, 3763.

[47] Y. J. Yu, S. Schreiner, L. Vaska, *Inorg. Chim. Acta*, **1990**, *170*, 145.

[48] R. T. Tom, A. S. Nair, N. Singh, M. Aslam, C. L. Nagendra, R. Philip, K. Vijayamohanan, T. Pradeep, *Langmuir*, **2003**, *19*, 3439.

[49] K. G. Thomas, J. Zajicek, P. V. Kamat, *Langmuir*, **2002**, *18*, 3722.

[50] G. Li, M. Lauer, A. Schulz, C. Boettcher, F. Li, J.-H. Fuhrhop, *Langmuir*, **2003**, *19*, 6483.

[51] C. Lofton, W. Sigmund, *Adv. Funct. Mater.*, **2005**, *15*, 1197.

[52] C. Besson, E. E. Finney, R. G. Finke, *J. Am. Chem. Soc.*, **2005**, *127*, 8179.

[53] C. Besson, E. E. Finney, R. G. Finke, *Chem. Mater.*, **2005**, *17*, 4925.

[54] M. A. Watzky, R. G. Finke, *Chem. Mater.*, **1997**, *9*, 3083.

[55] M. A. Watzky, R. G. Finke, *J. Am. Chem. Soc.*, **1997**, *119*, 10382.

[56] H. W. Liao, J. H. Hafner, *J. Phys. Chem. B*, **2004**, *108*, 19276.

[57] D. G. Duff, A. Baiker, P. P. Edwards, *Langmuir*, **1993**, *9*, 2301.

[58] A. V. Gaikwad, G. Rothenberg, *Phys. Chem. Chem. Phys.*, **2006**, *8*, 3669.

[59] A. E. Saunders, M. B. Sigman, Jr., B. A. Korgel, *J. Phys. Chem. B*, **2004**, *108*, 193.

[60] J. M. Petroski, Z. L. Wang, T. C. Green, M. A. El-Sayed, *J. Phys. Chem. B*, **1998**, *102*, 3316.

[61] Q. Jiang, H. M. Lu, M. Zhao, *J. Phys: Cond. Matter*, **2004**, *16*, 521.

[62] T. H. Ha, H.-J. Koo, B. H. Chung, *J. Phys. Chem. C*, **2007**, *111*, 1123.

[63] O. M. Magnussen, *Chem. Rev.*, **2002**, *102*, 679.